ELSEVIER

Journal of Nuclear Materials 301 (2002) 193–202

journal of nuclear materials

www.elsevier.com/locate/jnucmat

A new technique for the prediction of non-linear material behavior

J.A. Wang *, N.S. Rao

Oak Ridge National Laboratory, P.O. Box 2008, Building 6011, Oak Ridge, TN 37831-6370, USA

Received 17 April 2001; accepted 2 November 2001

Abstract

A new methodology is developed for the prediction of material behavior, such as aging processes, by utilizing a combination of domain models and non-linear estimators including neural networks and nearest neighbor regressions. This methodology is applied to the problem of predicting embrittlement levels in light-water reactors by combining the existing models with the conventional non-linear estimators. The Power Reactor Embrittlement Database is used in this study. The results indicate that the combined embrittlement predictor achieved about 56.5% and 32.8% reductions in the uncertainties for General Electric Boiling Water Reactor plate and weld data compared to Regulatory Guide 1.99, Revision 2, respectively. The implications of irradiation temperature effect to the development of radiation embrittlement model are then discussed.

1. Introduction

As we face the increasing electricity demand worldwide and increasing concern about atmospheric emissions, nuclear energy will be an important option within a broad energy portfolio for industrialized and developing nations. The success of reactor technology depends critically on the effective surveillance program to monitor the degradation of irradiated materials during service. The aging and degradation of light-water reactor pressure vessels (RPVs) are of particular concern because the magnitude of the radiation embrittlement is extremely important to the plant's safety and operating cost. Property changes in materials due to neutron-induced displacement damage are a function of neutron flux, neutron energy, and temperature, as well as the pre-irradiation material history, material chemical composition and microstructure, since each of these influence radiation-induced microstructural evolution. These factors must be considered to reliably predict RPV embrittlement and to ensure the structural integrity of the RPV. Based on the embrittlement predictions, decisions must be made concerning operating parameters, low-leakage-fuel management, possible life extension, and the potential role of pressure vessel annealing. Therefore, the development of embrittlement prediction models for nuclear power plants (NPPs) is a very important issue for the nuclear industry regarding the safety and lifetime extension of aging commercial NPPs.

Service failures due to inaccurate characterization of material aging responses could result in potentially costly repairs or premature component replacements, and in a worst-case could result in a catastrophic failure and loss of life. The general degradation mechanisms of the material aging behavior can be quite complicates and include: microstructure and compositional changes, time-dependent deformation and resultant damage accumulation, environmental attack and the accelerating effects of elevated temperature, and synergistic effects of all the above. These complex non-linear dependencies make the modeling of aging material behaviors a difficult task.

There have been several domain models that capture various aspects for the material behavior; these models

* Corresponding author.
E-mail address: wangja@ornl.gov (J.A. Wang).

0022-3115/02/$ - see front matter
PII: S0022-3115(01)00750-4

are designed by the domain experts to capture various critical relationships. At the same time, conventional non-linear estimators – while requiring very limited domain expertise – can model relationships that are not readily apparent. Consequently, there has been a profusion of methods with complementary performance with no single method proven to be always better than all others. Our goal is to develop an effective methodology by combining the domain models with the non-linear estimators including, neural networks and nearest neighbor regressions (NNRs) to exploit their complementary strengths. We have previously developed a large Power Reactor Embrittlement Database (PR-EDB) [1] for US NPPs. Subsequently in cooperation with the Electric Power Research Institute, additional verification and quality assurance of the data were performed by the US reactor vendors. PR-EDB is used in this study to predict the embrittlement levels in light water RPVs. The results indicate that our combined predictor achieved about 56.5% and 32.8% reductions in the embrittlement uncertainties for General Electric (GE) Boiling Water Reactor (BWE) plate and weld data compared to Regulatory Guide 1.99, Revision 2, respectively.

More generally, this methodology offers a potential for a new research field in material science for the development of advanced materials through an understanding and/or modeling of the underlying mechanisms of material aging. In particular, this approach holds a promise for advances in material damage prediction of structural components as, for example, in the development of regulatory guidelines for managing surveillance programs regarding the integrity of nuclear reactor components.

In Section 2, we provide the background for the proposed methodology. The objectives are presented in Section 3. Various embrittlement models are briefly described in Section 4. The fusion method is described in Section 5, and the performance results are discussed in Section 6.

2. Background

The complex non-linear dependencies observed in typical material embrittlement data, as well as the existence of large uncertainties and data scatter, make the modeling of material behavior (such as embrittlement prediction) a difficult task. The conventional statistical and deterministic approaches have proven to result in large uncertainties, in part because they do not fully exploit the domain specific knowledge. The domain models built by researchers in the field, on the other hand, are not able to fully exploit the statistical and information content of the data. As evidenced in previous studies, it is unlikely that a *single* method, whether it is statistical, non-linear or domain model will outperform all others. Considering the complexity of the problem, it is more likely that certain methods will perform best under certain conditions. In this paper, we propose to combine a number of methods such as domain models, neural networks, and NNRs. The combined system has the potential to perform at least as well as the best of the constituents by exploiting the regions where the individual methods are superior. Such combination methods became possible due to recent developments in the measurement-based optimal fusers [2–4] in the area of information fusion.

The problem of estimating non-linear relationships from noisy data has been well studied in the area of statistical estimation [5]. The non-linear statistical estimators such as the Nadaraya–Watson estimator and regressograms [6] essentially rely on the properties of regressions. While neural networks and statistical estimators are general, the domain models developed by the material scientists specifically capture the critical relationships in the data that are not easily amenable to general methods. Such models are typically based on a combination of linear and non-linear models, which are carefully chosen through an understanding of experimental data.

Particularly among the models developed for embrittlement data, there is unlikely to be a single winner, and different models perform well under different conditions. By discarding one or more models, one stands the risk of not characterizing certain critical performance. We propose to combine various methods using isolation fusers [5]. The most important part of these fusers is that the combined system can be guaranteed to be at least as good as the best individual estimator with a specified probability. Furthermore, fusion of no proper subset of the models performs better than the fused system based on all models. This way the positive aspects of *all* individual estimators can be exploited without discarding any single estimator.

We now briefly illustrate the overall fusion method to highlight the underlying principle. Consider the following target function, wherein the objective it to model this function using the training data points obtained by knowing the function values at certain values of x. The prediction of each model is then tested using test data points that are different from the training points. We consider different estimators based on artificial neural networks (ANN), where each estimator has a different number of hidden nodes and different learning rate for the backpropagation training algorithm.

$$f(x) = 0.02(12 + 3x - 3.5x^2 + 7.2x^3)(1 + \cos 4\pi x) \times (1 + 0.08 \sin 3\pi x). \quad (1)$$

Consider that we obtain six different neural network estimators for the target function by randomly choosing

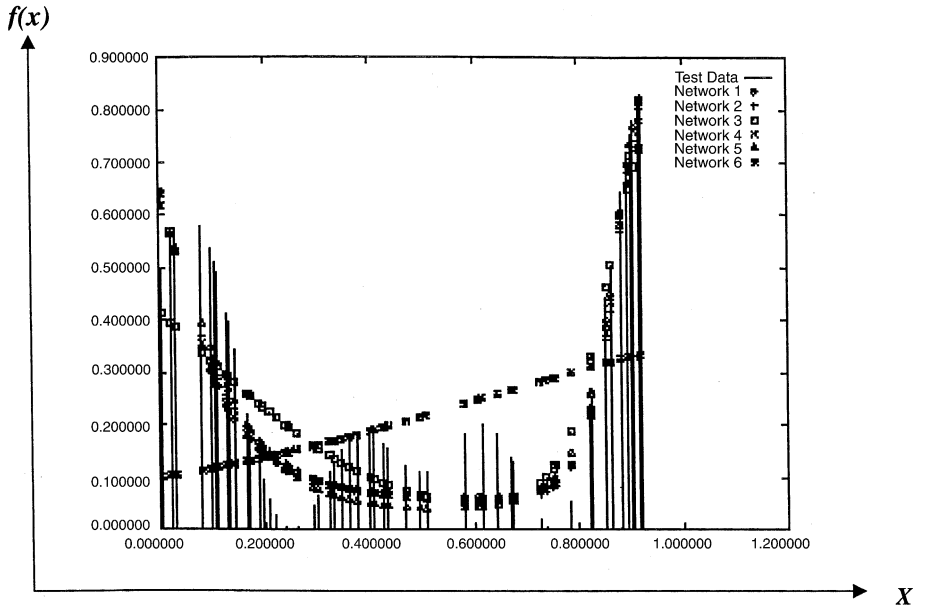

Fig. 1. Six ANN prediction models trained with backpropagation algorithm with different learning rates randomly chosen.

the number of hidden nodes and the learning rate parameters for the backpropagation algorithm. Each neural network is trained with the same set of sample points and tested on set of test points. The predictions of the networks on the test data points are shown in Fig. 1. The solid lines represent the actual function values, and predictions by different neural networks are shown by various other symbols. It is of interest to note that network 4 appears to be a linear fit and the worst fit among all networks. But, it is the only network that is able to accurately model the function $f(x)$ at the neighborhood of $x = 0.4$. We now combine the results using linear and projective fusers, both of which are special cases of the isolation fusers; their performance is shown in Fig. 2. The linear fuser's output is shown in dotted lines and the output of projective fuser is denoted by $+$. Compared to the actual function values (test data), both fusers perform similarly except around $x = 0.4$. The projective fuser identified that one of the neural network 4 performs better than other in this regions and utilized to predict the function. Note that this is the only region that this neural network performed well, and projective fuser is able to exploit its superior performance in this localized region. In terms of test error, the linear fusers is 31.15 times better than best ANN estimator and the projective fuser is 1.3 times better than linear fuser. The summary of these results is presented in Table 1, which shows that carefully chosen fusers can achieve performance significantly better than the individual estimators. In essence, both fusers are able to achieve performance superior to the individual estimators by 'exploiting' the performances of the individual estimators. In particular, both fusers are shown to perform at least as good as the best of the estimators (in terms of the test error).

For the embrittlement problem, the deployment of these fusers on various models will ensure that the fused model is at least as good as the best of the individual models, irrespective of their individual performances. However, the general results on fusers do not specify the actual performance gains that may be achieved in a particular application. We show here that significant performance improvements are indeed obtained by employing fusers to combine various embrittlement models.

3. Objectives

Our objective is to combine various estimators for predict the embrittlement behavior of irradiated materials, and then combine them to exploit their complementary strengths. We employ neural networks, NNRs, and domain models, based on the PR-EDB data, to predict the transition temperature shift of RPV materials, which is a measure of the material embrittlement. From the past experience [7], the boiling water has larger uncertainty compared to the other power reactor data. In this study, we only focused on the BWR data.

The first task is to create unbiased training and test sets. The GE BWR surveillance data (listed in PR-EDB) were pre-processed and streamlined. The final processed

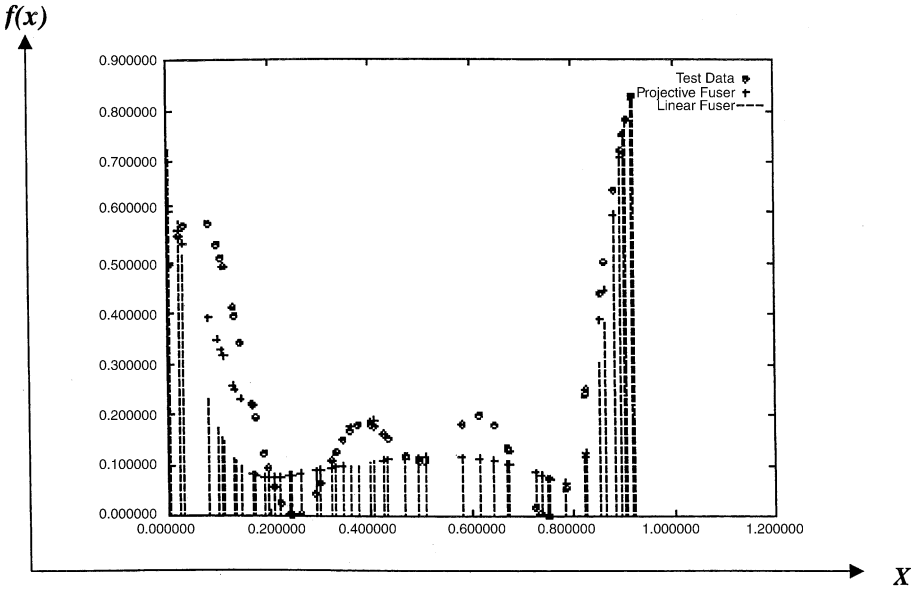

Fig. 2. Two information fusion models. In terms of test error, the linear fusers is 31.15 times better than the best ANN, and the projective fuser is 1.3 times better than the linear fuser.

Table 1
Summary of the simulation results for the information fusion technique

Data size		Projective as good[a]	Other better		Performance (times)[b]		Average error
Training	Test		Linear	Best	Linear	Best	
Without noise							
10	10	8	1	1	1.009269	10.489711	0.075042
25	25	8	2	0	1.039885	13.426878	0.021926
50	50	10	0	0	1.304039	31.157175	0.013454
75	75	10	0	0	1.530556	89.050201	0.004725
100	100	10	0	0	1.788104	87.905518	0.003764
With noise							
10	10	8	2	0	0.982823	9.205843	0.041874
25	25	8	2	0	1.045973	14.115362	0.026983
50	50	10	0	0	1.293410	19.121033	0.010399
75	75	9	1	0	1.275850	33.192585	0.008435
100	100	10	0	0	1.227069	37.937778	0.007115

[a] For each dataset size, 10 different samples are utilized.
[b] Projective fuser outperformed both linear fuser and the best estimators.

GE BWR data were compared with that of the ASTM E10.02 subcommittee embrittlement database for consistency in the surveillance information, such as irradiation temperature, chemical composition, Charpy impact test data fitting methodology, and power time history, etc. The processed GE BWR data have essentially the same neutron fluences, chemistry, and irradiation temperature data compared to those of ASTM E10.02 database, with minor difference of transition temperature shift (within a few degree F). The GE BWRs data values were then scaled to the interval $[-1,1]$ using a Linear Max/Min transformation. This ensures that no one component in the data dominates the parameter optimization scheme. Then the data were randomly partitioned into training and testing sets.

The second task consists of determining a number of estimators for this problem. For each method, a criteria function and optimization routine will be selected that consistently produces stable results. For statistical estimators, we will follow the procedure described in the

literature. For ANN, one hidden layer and eleven hidden nodes were chosen with 2000 epoch iteration. A random generator was used to generate the initial weights for ANN modeling. Four sets of ANN models were tested. We then combine the statistical and deterministic estimators using information fusion techniques. The combined system is guaranteed to perform at least as well as the best of the constituents by exploiting the regions where the individual methods are superior.

A novel methodology is developed here for inferring non-linear relationships that are typical in material behavior prediction. A tool based on this methodology is also implemented for the embrittlement prediction of NPPs. This tool could be expanded and adapted for use in other areas in which non-linear material properties are important, such as failure analysis of highway bridges, airplane safety analyses, and others.

4. Embrittlement prediction models

In this section we briefly described various models used for embrittlement prediction, which will be combined in the next section.

4.1. ORNL embrittlement prediction models

The residual defects in materials due to neutron-induced displacement damage are a function of neutron energy, neutron flux, exposure temperature, and the material properties that determine how neutrons interact with atoms and how defects interact within the material [8]. Thus, temperature, neutron flux, neutron energy spectrum, and material composition and processing history all contribute to the radiation embrittlement process [9]. Insufficient considerations of these factors may result in misleading correlations and, thus, incorrect predictions of material state and material behavior, as well as incorrect end-of-life determinations.

To minimize the influences of the uncertainty of the irradiation temperature, neutron energy spectrum, displacement rate, and plant operation procedures on embrittlement models, improved embrittlement models based on group data that have similar radiation environments and reactor design and operation criteria are examined. The development of new embrittlement prediction equations [7,10] stem from a series of studies on radiation embrittlement models, such as Guthrie's model [11], Odette's model [12], Fisher's model [13], B&W Lowe's model [14], the French FIM model [15], etc., and several other parameter studies on the PR-EDB. Although the copper-precipitation model has been extremely successful in explaining many aspects of irradiation embrittlement, it is becoming increasingly evident that other elements also contribute to the embrittlement of the RPV steel, such as Ni, P, Mn, Mo, and S. Theoretically, all the impurities in low alloy steel are candidates to be included in the modeling. For example, C, Si, Mn, Mo, S, etc., were investigated in the test run, but including or excluding these elements did not affect the overall outcome of the statistical parameters significantly; therefore, these parameters (or elements) were not incorporated into final governing equations. Thus, Cu, Ni, and P were tentatively selected as key elements and were incorporated into the formula of the new prediction equations. Furthermore, the reason for separating weld and base metals is because the welds tend to show the enhanced degradation. And the welding process presents a possible region of physical and metallurgical discontinuity, and offers added chances for the introduction of defects and undesirable components or stresses.

A non-linear-least-squares fitting Fortran program was written for this study. The development of the parameters for this new embrittlement model is based on statistical formulation chosen by computer iterations. To some extent, the physical mechanisms are embedded in the equations, such as the formulation of the fluence factor (FF). Two new prediction models for GE BWRs data were developed, where the fluence rate effect was considered in the second prediction model, and are described below:

Model 1

$$\begin{aligned}\Delta\mathrm{RTNDT}\ (\mathrm{base}) &= [-94.8 + 411.9\mathrm{Cu} + 247.3\sqrt{\mathrm{CuNi}} \\ &\quad + 498\mathrm{P/Cu}]f^{0.3216-0.001003\ln f}, \\ \Delta\mathrm{RTNDT}\ (\mathrm{weld}) &= [420.9\mathrm{Cu} + 134.6\sqrt{\mathrm{CuNi}} \\ &\quad - 25.94\mathrm{P/Cu}]f^{0.2478-0.01475\ln f}. \end{aligned} \quad (2)$$

Model 2

$$\begin{aligned}\Delta\mathrm{RTNDT}\ (\mathrm{base}) &= \Big[(13.62 + 318.1\mathrm{Cu} - 58.75\sqrt{\mathrm{NiCu}} \\ &\quad - 151.4\mathrm{P/Cu})f^{-0.4354-0.1285\ln f}\Big] \\ &\quad + \Big[(18.44 - 49.13\sqrt{\mathrm{CuNi}} - 17.22\mathrm{Cu} \\ &\quad - 97.57\mathrm{P/Cu})f(-8.344 \\ &\quad - 0.7045\ln f)\ln(t_i/600000)\Big], \\ \Delta\mathrm{RTNDT}\ (\mathrm{weld}) &= 1.075\Big[(1580\mathrm{Cu} - 86.06\sqrt{\mathrm{NiCu}} \\ &\quad + 43.55\mathrm{P/Cu})f^{0.6523+0.02866\ln f}\Big] \\ &\quad - 2.23[(4.193\mathrm{Ni} - 45.54\mathrm{Cu})f(-11.63 \\ &\quad - 0.4554\ln f)\ln(t_i/600000)], \end{aligned} \quad (3)$$

where ΔRTNDT is the transition temperature shift in °F; and neutron fluence f is in unit of 10^{19} n/cm^2 ($E > 1$ MeV), effective full power time, t_i, is in hour, and Cu, Ni, P are in wt%.

4.2. Regulatory Guide 1.99, Revision 2's model

The transition temperature shift of Reg. Guide 1.99, Rev. 2's model [16] was also used in this study for comparison purpose, which is described as below.

$$\Delta RT_{NDT} = (CF) f^{(0.28-0.10\log f)}, \tag{4}$$

where ΔRT_{NDT} is the transition temperature shift in °F, CF (°F) is the chemistry factor (given in the Table 1 and Table 2 of Reg. Guide 1.99, Revision 2), which is a function of copper and nickel content, and neutron fluence f is in unit of 10^{19} n/cm^2 ($E > 1$ MeV).

The residuals, defined as 'measured shift minus predicted shift,' for Reg. Guide 1.99, Rev. 2's model are illustrated in Figs. 3 and 4 for base and weld, respectively.

4.3. Eason's models

The developed embrittlement model by E.D. Eason et al. (Eason's model) [17], was used in this study. The

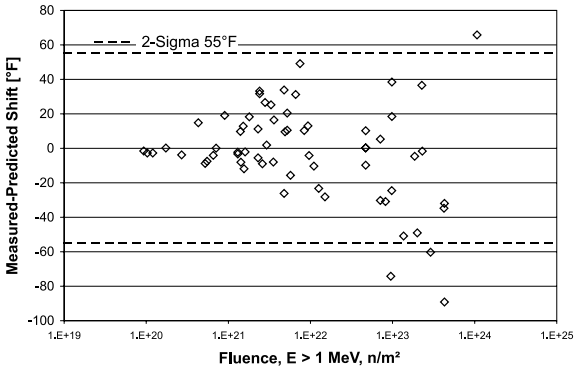

Fig. 3. Regulatory Guide 1.99, Revision 2's residual for GE BWR plate materials.

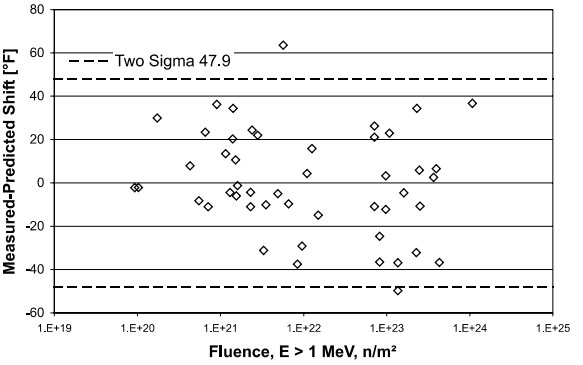

Fig. 4. Regulatory Guide 1.99, Revision 2's residual for GE BWR weld materials.

Eason's trend curve of transition temperature shift was developed based on the power reactor data, and is described below.

$$\Delta T_{30p} = ff_1(\phi t) + ff_2(\phi t) f(cc) \quad [°F],$$

$$ff_1(\phi t) = A \exp\left[\frac{1.906 \times 10^4}{T_c + 460}\right](1 + 57.7P)\left[\frac{\phi t}{10^{19}}\right]^a,$$

$$ff_2(\phi t) = \frac{1}{2} + \frac{1}{2}\tanh\left[\frac{\log(\phi t + 5.48 \times 10^{12} t_i) - 18.29}{0.600}\right],$$

$$ff(cc) = B(\mathrm{Cu} - 0.72)^{0.682}(1 + 2.56\mathrm{Ni}^{1.358}), \tag{5}$$

where

$$a = 0.4449 + 0.0597\log\left[\frac{\phi t}{10^{19}}\right], \quad \phi t = \text{fluence}.$$

Welds: $A = 1.10 \times 10^{-7}$, $B = 209$; plates: $A = 1.24 \times 10^{-7}$, $B = 172$; forgings: $A = 0.90 \times 10^{-7}$, $B = 135$; T_c is coolant inlet temperature, °F.

The residual of Eason's model are illustrated in Figs. 5 and 6 for base and weld, respectively.

Table 2
Two-sigma uncertainty of the embrittlement models for GE BWR data

Embrittlement model	Parameters					Two sigma of residual (°F)	
	Cu	Ni	ϕt	t_i	T_c	Base (64 points)	Weld (48 points)
Reg. Guide 1.99, Rev. 2	×	×	×			55.0	47.9
ORNL fuser Model I	×	×	×	×	×	23.9	32.2
ORNL fuser Model II	×	×	×	×		24.6	34.1
ORNL Model I	×	×	×			39.6	41.8
ORNL Model II	×	×	×	×		27.6	38.5
Eason's model	×	×	×	×	×	40.9	51.0
K-NNR model	×	×	×	×	×	39.1	41.4
ANN-4 model	×	×	×	×	×	56.4	78.8[a]

[a] | Residual | > 100 °F are not included in two-sigma uncertainty evaluation.

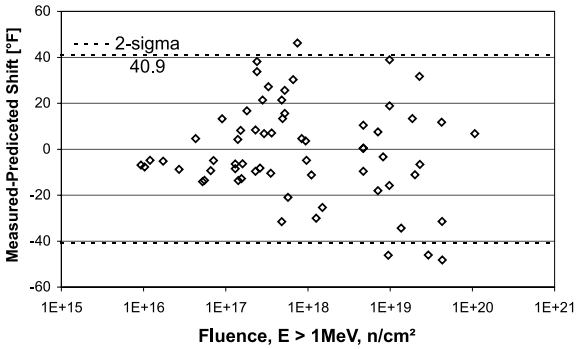

Fig. 5. Eason model's residual for GE BWR plate materials.

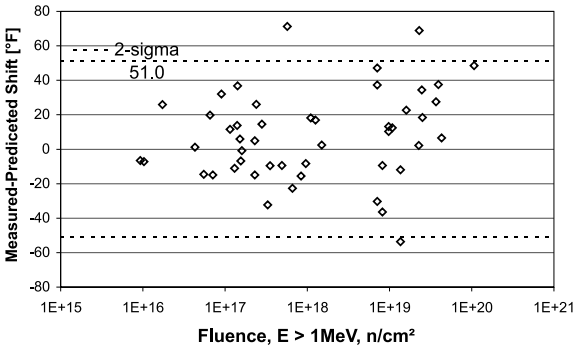

Fig. 6. Eason model's residual for GE BWR weld materials.

4.4. ANN models

An ANN is a parameterized non-linear mapping from an input space to an output space [18]. An ANN realizes mapping from an m-dimensional input space to an n-dimensional output space, and will have m nodes in its input layer and n nodes in its output layer. A multilayer ANN (ML-ANN) is the most common architecture. This architecture has additional layers of nodes between the input and output layers. The information from each input-layer node is fanned out to nodes in the layer hidden between the input and output layers. The information entering a node in any hidden or output layer is the weighted sum of all information leaving the layer below it in the hierarchy. The node performs a transformation on the weighted information it receives and fans out the result to all nodes in the layer above it in the hierarchy (except for the output layer). The weighting factors (weights) are free parameters that must be adjusted to some chosen criteria function using some optimization algorithm. In this way, ANNs are able to capture many higher-order correlations that may exist in the data. The relationship between the higher-order correlations produces a non-linear mapping. This is the reason ANNs may offer a more accurate prediction of material behaviors, embrittlement in this case. With methods like ANNs, one has a better tool to extract non-linear relationships from embrittlement data to aid in the development of reliable maintenance and safety strategies and regulations in the nuclear industry.

The backpropagation algorithm is used to train the network with the data [18]. The training process determines the weights of ANN to fit a suitable non-linear map. The backpropagation's flexibility of ANN is why it does a better job of modeling than linear regression, but this method has several weaknesses. The backpropagation algorithm is based on local descent and can get stuck in local minima, and as a result the predictive properties can be quite varied. Also, there are a number of tunable parameters such as starting weights and learning rates that have a significant effect on the weight computed by the back propagation algorithm. Thus, when different ANN models are trained with the same back propagation algorithm but with different starting weights and learning rates, the performance can be significantly different, as shown in Figs. 1 and 2. These networks however can be fused to achieve the performance of the best ANN [3].

Six independent variables, namely, Cu, Ni, P, fluence, irradiation temperature, and effective full power time were used in the ANN models. A program written in C language was used in this study.

4.5. K-nearest neighbor regression method

The NNR [5] is also chosen to generate an embrittlement model. The algorithm is described below. Let x_1, x_2, x_3,..., x_n be a sequence of n independent measurements with known classifications, and x be the measurement to be classified. Among x_1, x_2, x_3,..., x_n, let the measurement with the smallest distance from x be denoted as x'. Then the nearest-neighbor decision rule assigns the classification of x' to that of x. As for K-nearest neighbor regression (K-NNR), it assigns to an unclassified sample point the class most heavily represented among its K nearest neighbors to x. In this study we chose the first three nearest neighbors with properly weighted function to represent the unclassified sample.

Six independent variables, namely, Cu, Ni, P, fluence, irradiation temperature, and effective full power time were used in K-NNR models. A second test K-NNR model, excluding irradiation temperature from the fitting parameter, generated a nearly identical trend curve as that with irradiation temperature. A program written in C language was used in this study.

5. Fusion of embrittlement models

The development of this model consists of identifying the error profiles of various estimators and the physical

parameters of the underlying problem, and designing the fusers for combining the individual estimators. Here we combined the statistical and deterministic estimators using the linear fuser, which is a special case of the isolation fusers [19]. The isolation fusers are shown to perform probabilistically as good as best estimator [4,19]. Given n estimators, $f_1(x), \ldots, f_n(x)$, the linear fuser is given by $f(x) = w_1 f_1(x) + \cdots + w_n f_n(x)$, where $w_1, \ldots, w_n$ are the weights. We computed the weights for the fuser by minimizing the error of the fuser for the training set. The program was written in C where the solution is based on solving a quadratic programming problem. In this study, we utilized the linear fuser to develop the embrittlement models, six parameters, namely, Cu, Ni, P, fast fluence, irradiation time, and irradiation temperature, were incorporated into model development.

5.1. ORNL fuser model I

Eight different models were investigated including four neural network models, two ORNL models, one K-NNR method, and the Eason's model. The results of the ORNL linear fuser model indicate that this newly developed embrittlement model has about 56.5% and 32.8% reductions in uncertainties for GE BWR base and weld data, respectively, compared to that of Reg. Guide 1.99, Rev. 2. These are significant improvements on the embrittlement predictions for the RPV steels. The plots of information model residual and its two-sigma uncertainties for base and weld materials are illustrated in Figs. 7 and 8, respectively.

5.2. ORNL fuser model II

Fuser model II is a simplified version of fuser model I, excluding the irradiation temperature from the fitting parameter, and excluding the Eason's model from the fusion modeling. The data scatter of residuals for fuser model II are essentially the same as that of fuser model I. The results of ORNL fuser model II indicate that it has about 55.2% and 28.8% reduction in uncertainties for GE BWR base and weld data, respectively, compared to that of Reg. Guide 1.99, Rev. 2's model. This indicates that fuser model I has marginal improved performance compared to that of fuser model II. Thus, the impact of irradiation temperature on embrittlement modeling for GE BWRs surveillance data can be considered as secondary.

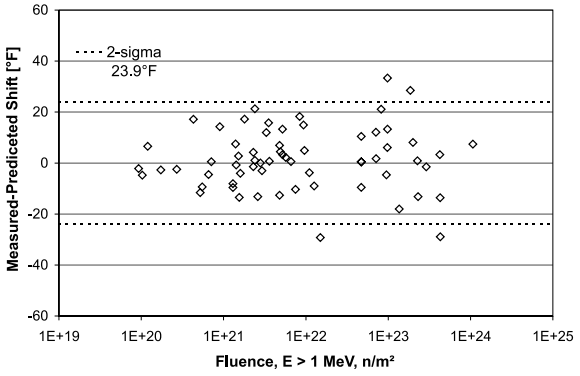

Fig. 7. ORNL-fuser model I overall residual for GE BWR base materials.

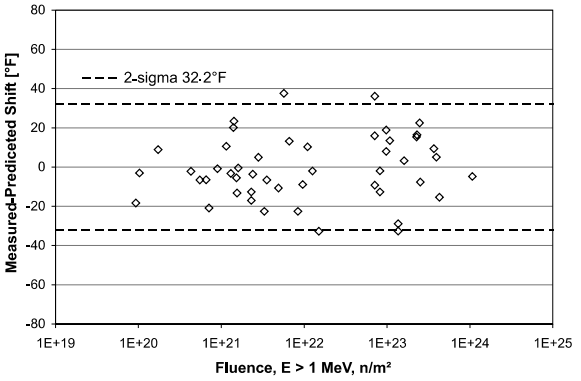

Fig. 8. ORNL-fuser model I overall residual for GE BWR weld materials.

6. Discussion

The comparison of the performance of the embrittlement models, based on the two-sigma uncertainty of residual values, is stated in Table 2. The fuser model gave the best performance among all the embrittlement prediction models. ORNL embrittlement models indicates that ORNL model II is superior to ORNL model I by including irradiation time to simulate fluence-rate effect. Thus, the implication of a flux effect in BWR environment was revealed in the model development.

The authors would like to point out that the fusion modeling developed here is based on G.E. BWR data, including 110 available sample data, where Reg. Guide 1.99/R2 and Eason's model were developed based on both PWR and BWR surveillance data. Thus, the superior prediction by ORNL fusion model comparing to that of Reg. Guide 1.99/R2 and Eason's models may also partially due to the subset of power reactor data used in the model development. However, in the same token, this study may also demonstrate the superiority and advantage of using subset data, for example, the vendor specific data, to develop power reactor embrittlement model. (The reason is explained in the next

paragraph.) In general a large data set with similar characteristics or controllable parameters will generate a better trend prediction compared to its subset. But a misleading trend curve can result from a large data set built upon different bases and uncontrollable parameters, revealed by its large uncertainty.

The R.G. Guide 1.99/R2 was formulated based on Guthrie's model and Odette's model and no temperature effect was considered in embrittlement models development, where, the FF and plates' chemistry factor (CF) are from Guthrie's model [16]. 177 surveillance data were used in Guthrie's model development; however, only 6 data are from BWR environment. Thus, BWR surveillance data may not be properly characterized from Reg. Guide 1.99/2's model. From ASTM E10.02 database, the mean temperature and one standard deviation of BWR and PWR data are 540.3 ± 13.6 and 545.7 ± 10.4 °F, respectively. Therefore, from the irradiation temperature variability point, the sample temperature environment of PWR and BWR are comparable. Currently, there are four major commercial power reactor vendors in the US, namely, Westinghouse, General Electric, Babcock & Wilcox, and Combustion Engineering. Each vendor has its unique designs and specific operating procedures. There are significant problems associated with insufficient information, such as the detailed irradiation temperature of surveillance specimen and the thermal gradient within surveillance capsules, and the lack of data in particular regions of interests to characterize the vendor's service environments. About 64% of PR-EDB data is from Westinghouse; thus, the trend curve of all the four vendors' data will closely resemble the Westinghouse plants' environment. Furthermore, B&W surveillance data appears to experience higher irradiation temperature (based on capsule melting wire) compared to other vendors, by combining low and high temperature data may further embedded bias on top of bias from the modeling point. For example, from the trend curve of all the vendors' data, the higher irradiation temperature data shows negative bias (i.e. prediction model shows over-prediction) and low irradiation data show positive bias. However, the overall bias (or uncertainty) will cancel each other resulting in a misleading statistical outcome, such as its means and uncertainty.

Eason's model covers both PWR and BWR environment, where 96 BWR data were included in model development, and coolant inlet temperatures were incorporated into governing equations to simulate temperature effect. In practice the coolant inlet temperature is incorporated into the embrittlement model to simulate the irradiation temperature for a pressurized light-water reactor. However, a past study [9] showed that a large bias can still be identified in Eason's model for surveillance data from a higher irradiation temperature environment, and the bias is similar to that of Regulatory Guide 1.99, Rev. 2. [16]. This may indicate that the coolant inlet temperature is not equivalent to the irradiation temperature experienced by the surveillance specimens. Furthermore, from this study on fuser models, neither including coolant inlet temperature or excluding coolant inlet temperature has a significant impact on the trend curve, which may further support the above statement.

It is of interest to note that ORNL model I and K-NNR model have very similar performance, however, K-NNR model is generated more straightforward without major efforts of refinement and reformulation of the governing equation compared to that of ORNL Model I.

For surveillance data, significant deviations of the measured shift from the trend curve (i.e., more or less than 34 °F for plate materials) should be considered as a warning flag pointing to a possible anomalous capsule environment. The large uncertainties are the result of errors in the overall environment description. But, limit attention has been given to characterizing the irradiation temperature environment of the surveillance specimens. In general, the neutron environment, fluence and flux, can be determined fairly accurately, and possible effects from these sources are relatively small in a power reactor environment. However, the surveillance capsules' temperature environments still heavily rely on the melting wire's measurement. A more detailed analytical investigation of specimen temperature is needed, based on detailed neutronic and thermal-mechanical analysis for specific capsule and specimen loading configuration, to facilitate the RPV surveillance program in confidence. Thus, in the current trend curve development, the most likely reason for deviations from the trend curve is the specimen temperature.

To develop a global embrittlement model for US power reactors, an independent investigation of each subgroup (each vendor) is recommended. Upon completing the investigations, if substantial improvement is achieved for each subset based on the proposed methodology, then information fusion technique will be utilized to integrate all the subset models into a global RPV embrittlement model.

7. Conclusions

We described an information fusion method for the embrittlement prediction in light water RPVs, by combining domain models with neural networks, and nearest neighbor regressions. Our method resulted in 56.5% and 32.8% reduction in 2-sigma uncertainties compared to that of the Reg. Guide 1.99, Rev. 2's model, for base and weld materials, respectively. This approach proved better than the ORNL embrittlement models and other conventional models.

This new approach combines the conventional non-linear methods and model based methods into an integrated methodology applicable for modeling material aging processes. This approach can potentially assist the nuclear industry on the issues regarding safety and life-time extension of aging commercial NPPs. By using a wide spectrum of methods, the proposed tool can potentially handle the subtle non-linearities and imperfections, and can serve as a calibration and benchmark for the existing models. The predictions generated by our system have the potential for providing efficient, reliable, and fast results, and can be an essential part of the overall safety assessment of material aging research.

Future improvements of the proposed method can be made through the development of the projective fusers [3], which are based on a projective space that depends on the underlying physical parameters. This class of fusers is based on the lower envelope of the error regression curves of various estimators such that the estimator that forms the envelope is utilized in that region.

Acknowledgements

The authors gratefully acknowledge the efforts of R.K. Nanstad for his valuable comments on this research. This research is sponsored by the R&D Seed Money Program of Oak Ridge National Laboratory, and by Engineering Research Program of Office of Basic Energy Sciences of US Department of Energy, under contract DE-AC05-00OR22725 with UT-Battelle, LLC.

References

[1] J.A. Wang, Embrittlement Data Base, Version 1, NUREG/CR-6506 (ORNL/TM-13327), US Nuclear Regulatory Commission, August 1997.
[2] N.S.V. Rao, J. Franklin Inst. 336 (2) (1999) 285.
[3] N.S.V. Rao, Multisensor fusion under unknown distributions: Finite sample performance guarantees, in: A.K. Hyder (Ed.), Multisensor Fusion, Kluwer, Dordrecht, 2001.
[4] N.S.V. Rao, IEEE Trans. Pattern Anal. Mach. Intell. 23 (8) (2001) 904.
[5] R.O. Duda, P.E. Hart, D.G. Stork, Pattern Classification, 2nd ed., Wiley, New York, 2001.
[6] N.S.V. Rao, V. Protopopescu, Proc. IEEE 84 (10) (1996) 1562.
[7] J.A. Wang, in: Development of Embrittlement Prediction Models for US Power Reactors, Effect of Radiation on Materials: 18th International Symposium, ASTM STP 1325, American Society for Testing and Materials, Philadelphia, March 1999, p. 525.
[8] L.K. Mansur, Mechanisms and kinetics of radiation effects in metals and alloys, in: G.R. Freeman (Ed.), Kinetics of Nohomogeneous Processes, Wiley, New York, 1987.
[9] J.A. Wang, in: Analysis of the Irradiated Data for A302B and A533B Correlation Monitor Materials, Effect of Radiation on Materials: 19th International Symposium_ASTM STP 1366, American Society for Testing and Materials, Philadelphia, March 2000, p. 59.
[10] J.A. Wang, F.B.K. Kam, F.W. Stallmann, in: Embrittlement Data Base (EDB) and Its Applications, Effects of Radiation on Materials: 17th Volume, ASTM STP 1270, American Society for Testing and Materials, Philadelphia, PA, 1996, p. 500.
[11] G.L. Guthrie, Charpy Trend Curves Based on 177 PWR Data Points, NUREG/CR-3391, US Nuclear Regulatory Commission, 1983.
[12] G.R. Odette, P.M. Lombrozo, J.F. Perrin, R.A. Wullaert, Physically Based Regression Correlations of Embrittlement Data From Reactor Pressure Vessel Surveillance Programs, EPRI NP-3319, Electric Power Research Institute, 1984.
[13] S.B. Fisher, J.T. Buswell, A Model for PWR Pressure Vessel Embrittlement, Berkeley Nuclear Laboratories, Central Electric Generating Board, GL139PB, 1986.
[14] A.L. Lowe Jr., J.W. Pegram, Correlations for Predicting the Effects of Neutron Radiation on Linde 80 Submerged-Arc Welds, BAW-1803, Rev. 1, May 1991.
[15] C. Brillaud, F. Hedin, B. Houssin, A Comparison Between French Surveillance Program Results and Predictions of Irradiation Embrittlement, Influence of Radiation on Material Properties, ASTM STP 956, 1987, p. 420.
[16] P.N. Randall, Basis for Revision 2 of the US Nuclear Regulatory Commissions Regulatory Guide 1.99, Radiation Embrittlement of Nuclear Reactor Pressure Vessel Steels: An International Review (Second Volume), ASTM STP 909, 1986, p. 149.
[17] E.D. Eason, J.E. Wright, G.R. Odette, Improved Embrittlement Correlations for Reactor Pressure Vessel Steels, NUREG/CR-6551, US Nuclear Regulatory Commission, 2000.
[18] M.H. Hassoun, Fundamentals of Artificial Neural Networks, MIT, Cambridge, MA, 1995.
[19] N.S.V. Rao, Finite sample performance guarantees of fusers for function estimators, in: Information Fusion, vol. 1 (1), 2000, p. 35.